

Supporting information

Fucosyltransferase-specific inhibition *via* next generation of fucose mimetics.

Kyle C. Martin,^{abc} Jacopo Tricomi,^d Francisco Corzana,^e Ana García-García,^f Laura Ceballos-Laita,^f Thomas Hicks,^g Serena Monaco,^g Jesus Angulo,^{ghi} Ramon Hurtado-Guerrero,^{fjk} Barbara Richichi^{d*†} and Robert Sackstein.^{abc*†}

^a Department of Translational Medicine, Translational Glycobiology Institute, Herbert Wertheim College of Medicine, Florida International University, Miami, FL 33199. Email: sackstein@fiu.edu

^b Department of Dermatology, Brigham and Women's Hospital, Harvard Medical School, Boston, MA 02115.

^c Program of Excellence in Glycoscience, Harvard Medical School, Boston, MA 02115.

^d Department of Chemistry 'Ugo Schiff', University of Florence, Via della Lastruccia 13, 50019 Sesto Fiorentino (FI). Email: barbara.richichi@unifi.it

^e Departamento de Química, Universidad de La Rioja, Centro de Investigación en Síntesis Química, 26006 Logroño, Spain.

^f Institute of Biocomputation and Physics of Complex Systems (BIFI), University of Zaragoza, Mariano Esquillor s/n, Campus Rio Ebro, Edificio I+D, Zaragoza, Spain; Fundación ARAID, 50018, Zaragoza, Spain.

^g School of Pharmacy, University of East Anglia, Norwich Research Park, NR47TJ, Norwich, UK.

^h Departamento de Química Orgánica, Universidad de Sevilla, C/ Prof. García González, 1, 41012 Sevilla, Spain.

ⁱ Instituto de Investigaciones Químicas (CSIC-US), Avda. Américo Vespucio, 49, 41092 Sevilla, Spain.

^j Copenhagen Center for Glycomics, Department of Cellular and Molecular Medicine, School of Dentistry, University of Copenhagen, Copenhagen, Denmark.

^k Laboratorio de Microscopías Avanzada (LMA), University of Zaragoza, Mariano Esquillor s/n, Campus Rio Ebro, Edificio I+D, Zaragoza, Spain.

* Corresponding: barbara.richichi@unifi.it; sackstein@fiu.edu

† BR and RS are co-last and co-corresponding authors.

Table of Contents

Figure S1	S2
Molecular dynamics (MD) simulations	S2
Figure S2	S3
Figure S3	S3
Exofucosylation of the RPMI-8402 cells line using FTVI and GDP-Fuc.	S3
Figure S4	S4
Antibodies, flow cytometric analysis	S4
Inhibition of exofucosylation of the RPMI-8402 and MSC cells using fucose mimetic 1.	S4
Parallel Plate Flow Chamber	S4
Expression of GFP-FTVI in HEK2936E cells	S5

Protein purification	S5
Saturation Transfer Difference (STD) NMR experiments	S5
Saturation Transfer Difference (STD) NMR experiments. Binding Epitope Mapping from Initial Slopes (STD build-up curves)	S5
Table S1	S6
Figure S5	S6
Figure S6	S7
Dynamic light scattering (DLS)	S7
Figure S7	S7
Figure S8	S8
Figure S9	S9
Figure S10	S10
Figure S11	S10
References	S11
Author contributions	S11
Acnowledgments	S11
Abbreviations List	S12

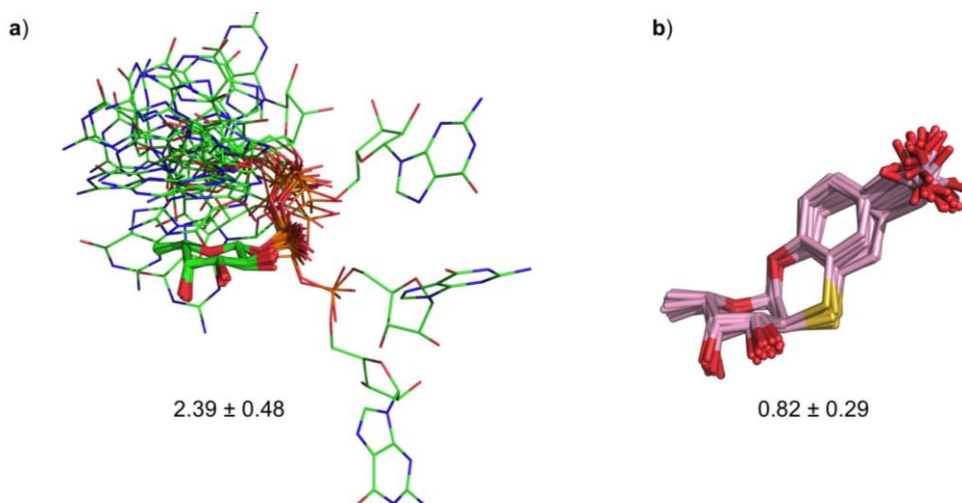


Figure S1. Structural ensembles derived from 1 μ s molecular dynamics (MD) simulations for GDP-Fuc **a)** and mimetic **1 b)** in water. Numbers indicate the RMSD values (heavy atoms) in \AA . Fucose residue in GDP-Fuc is shown as sticks.

Molecular dynamics (MD) simulations

Parameters for GDP-Fuc and mimetic **1** were generated with the antechamber module of Amber18,¹ using the general Amber force field (GAFF),² with partial charges set to fit the electrostatic potential generated with HF/6-31G(d) by RESP.³ The charges were calculated according to the Merz-Singh-Kollman scheme using Gaussian 09.⁴ Each compound was immersed in a water box with a 10 \AA buffer of TIP3P water molecules.⁵ The system was neutralized by adding explicit counter ions (Na^+). A two-stage geometry optimization approach was performed. The first stage minimizes only the positions of solvent molecules and ions, and the second stage is an unrestrained minimization of all the atoms in the simulation cell. The systems were then gently heated by incrementing the temperature from 0 to 300 K under a

constant pressure of 1 atm and periodic boundary conditions. Harmonic restraints of 30 kcal·mol⁻¹ were applied to the solute, and the Andersen temperature coupling scheme⁶ was used to control and equalize the temperature. The time step was kept at 1 fs during the heating stages, allowing potential inhomogeneities to self-adjust. Water molecules are treated with the SHAKE algorithm such that the angle between the hydrogen atoms is kept fixed. Long-range electrostatic effects are modelled using the particle-mesh-Ewald method.³³ An 8 Å cutoff was applied to van der Waals interactions. Each system was equilibrated for 2 ns with a 2-fs time-step at a constant volume and temperature of 300 K. Production trajectories were then run for additional 1 μs under the same simulation conditions.

Cell Type (Structure)	Comparison of Treatments	P value	Cell Type (Structure)	Treatment	P value
RPMI sLe ^x	FTVII vs 1:1	P < 0.01	MSC sLe ^x	FTVII vs 1:1	P < 0.05
	FTVII vs 1:2	P < 0.01		FTVII vs 1:2	P < 0.05
	FTVII vs 1:2 Pre	P < 0.01		FTVII vs 1:2 Pre	P < 0.01
RPMI Le ^x	FTIX vs 1:1	P > 0.05	MSC Le ^x	FTIX vs 1:1	P > 0.05
	FTIX vs 1:2	P > 0.05		FTIX vs 1:2	P > 0.05
	FTIX vs 1:2 Pre	P < 0.05		FTIX vs 1:2 Pre	P > 0.05
RPMI sLe ^x	FTVI vs 1:1	P < 0.05	MSC sLe ^x	FTVI vs 1:1	P < 0.05
	FTVI vs 1:2	P < 0.01		FTVI vs 1:2	P < 0.01
	FTVI vs 1:2 Pre	P < 0.01		FTVI vs 1:2 Pre	P < 0.01
RPMI Le ^x	FTVI vs 1:1	P < 0.05	MSC Le ^x	FTVI vs 1:1	P > 0.05
	FTVI vs 1:2	P < 0.01		FTVI vs 1:2	P < 0.01
	FTVI vs 1:2 Pre	P < 0.01		FTVI vs 1:2 Pre	P < 0.01

Figure S2. P value table for Figure 1 – Table contains P values for all reactions in Figure 1B. Statistical analysis was performed using one-way ANOVA, followed by Dunnett's multiple comparisons test where appropriate. For all above experiments n = 3.

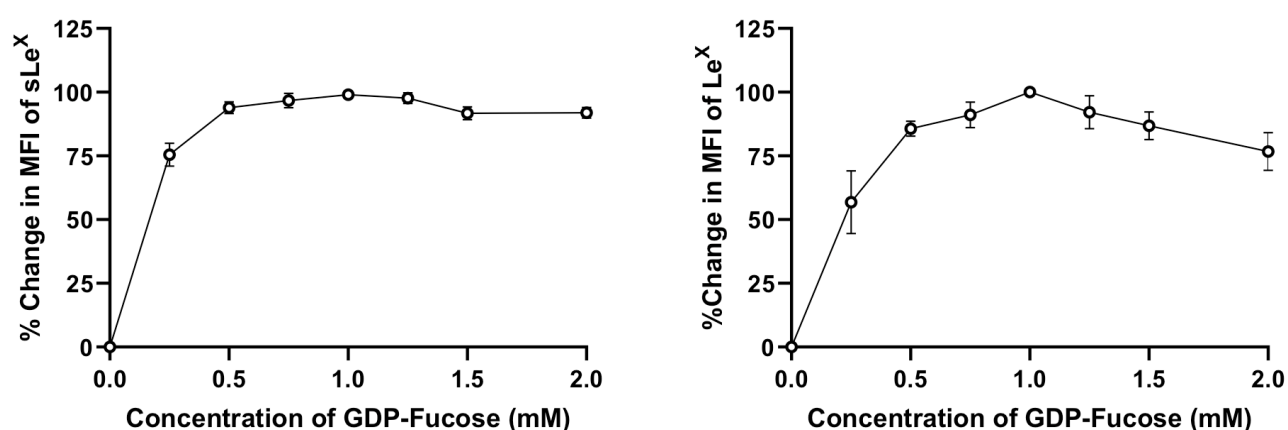


Figure S3. Exofucosylation of the RPMI-8402 cells line using FTVI. All reactions were carried out in triplicate using increasing concentrations of GDP-fucose and 1 x 10⁶ cells each.

Exofucosylation of the RPMI-8402 cells line using FTVI and GDP-Fuc.

A titration of GDP-fucose was carried out to determine the maximum mean fluorescent intensity (MFI) of sLe^x and Le^x *via* flow cytometry for downstream inhibition experiments. Generally, 1 x 10⁶ cells were used in each FTVI exofucosylation reaction and all reactions were carried out in

triplicate. Cells were then stained with either Alexa-Fluor 488 Mouse Anti-Human CD15s (BD Biosciences), or APC anti-human CD15 (SSEA-1) Antibody (BioLegend). Cells were then acquired on a Canto II (BD Biosciences) flow cytometer and analyzed using Flowjo software (Treestar). FTVI was purchased from R&D systems.

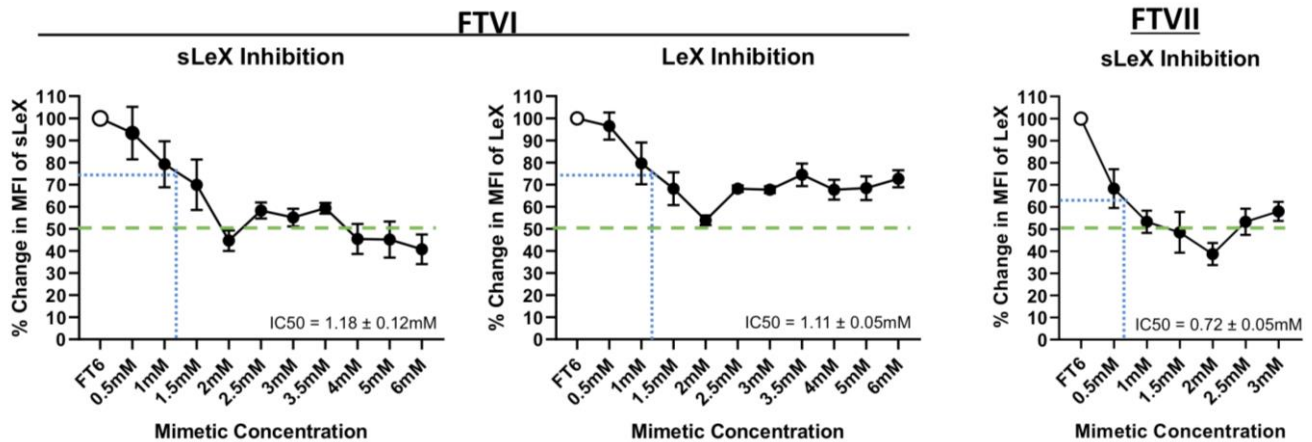


Figure S4. Inhibition of exofucosylation of the RPMI-8402 cells line using fucose mimetic 1. All reactions were carried out in triplicate utilizing 1.0 mM of GDP-fucose and 1×10^6 cells each. The green dotted line represents a 50% reduction in the creation of sLe^X and Le^X. The blue dotted lines represent the \sim IC₅₀ calculated values. IC₅₀ values were calculated from steady state rate regions (linear portions) of each curve, and represent the concentration of mimetic needed to inhibit 50% of the fucosyltransferase activity. This was then extrapolated from % change in MFI vs. mimetic 1 concentration. We used Microsoft Excel to obtain best fit and to calculate IC₅₀ values.

Antibodies, flow cytometric analysis.

A Canto II (BD Biosciences) flow cytometer was utilized for flow cytometry and the data acquired was analyzed using FlowJo Software (Treestar). Cells were stained using antibodies specific to sLe^X (Alexa-Fluor 488 Mouse Anti-Human CD15s (BD Biosciences)), or Le^X (APC anti-human CD15 (SSEA-1) Antibody (BioLegend)).

Inhibition of exofucosylation of the RPMI-8402 and MSC cells using fucose mimetic 1.

Cells of the RPMI-8402 cell line and MSC cell line were treated with either 0.3 μ g of fucosyltransferase VI (FTVI), 2.7 μ g of fucosyltransferase VII (FTVII), 1.0 μ g fucosyltransferase IX (FTIX) or buffer-only at 37 °C for 60 minutes. All reactions contained at 1×10^6 cells/30 μ l in HBSS with 10 mM Hepes, 0.1% Human Serum Albumin, and 1.0 mM GDP fucose (Carbosynth) and the appropriate fucosyltransferase. Then, mimetic 1 was added to each of the treatment groups in molar equivalents with respect to GDP-Fuc with each of the fucosyltransferases. The treatment groups were as follows: 1:1 GDP-Fuc to mimetic 1 (*i.e.*, 1.0 mM GDP-Fuc and 1.0 mM mimetic), 1:2 GDP-Fuc to mimetic 1 (*i.e.*, 1.0 mM GDP-Fuc and 2.0 mM mimetic), or preincubated in presence of FT with a 2.0 mM solution of the mimetic 1 for 45 minutes followed by addition of a 1.0 mM solution of GDP-Fuc for 1 hour. Concentrations of the various FTs were utilized that would maximize the MFI to allow the detection of the efficacy of mimetic 1 to inhibit the various enzymes.

Parallel Plate Flow Chamber

Human umbilical vein endothelial cells (HUVEC, Lonza) were cultured in Endothelial Cell Growth Media (R&D Systems) in Bioflux microfluidic chambers that had been previously coated with 250 μ g/ml fibronectin (BD Biosciences). Then 4 hours prior to rolling assay, cells were activated with 40 ng/ml TNF α (R&D Systems). Different cell subsets, based on exofucosylation/mimetic conditions, were then infused into the chamber at a concentration of 2×10^6 /ml and shear stress was applied from 0.5–8 dynes/cm². Then RPMI-8402 subsets were loaded into chambers containing monolayers of E-selectin bearing HUVECs with an initial shear rate of 0.5 dyne/cm², with stepwise increments in the shear rate up to 8 dynes/cm². The number of tethering/interacting RPMI-8402 cells on HUVEC were quantified at each shear rate and averaged across three different fields of view.

Expression of GFP-FTVI in HEK2936E cells

pGEN2-HsFUT6 was isolated and purified from *Escherichia coli* strain DH5 α using NucleoBond PC 10000 EF Gigaprep kit (Macherey-Nagel). HEK2936E suspension culture cells were grown to a cell density of $1-1,5 \times 10^6$ in FreeStyle F17 Expression Medium (Thermo Fisher Scientific) supplemented with 2% GlutaMax (Thermo Fisher Scientific) and 0,1% Kolliphor P188 (Sigma). The vector was transfected into cells using linear polyethylimine 'Max' (MW 40,000; Polysciences). The culture supernatant was harvest after 4 days of shaking the cells at 125 rpm, 37°C, 8% CO₂.

Protein purification

GFP-HsFTVI was purified from suspension culture medium by nickel-affinity purification using HisTrap HP (GE Healthcare) column connected to an ÄKTA FPLC system (GE Healthcare). The filtered culture medium was dialyzed overnight against 25 mM Tris pH 7.5, 150 mM NaCl, 10 mM Imidazole and injected into the column at 1.0 ml/min. The bound protein was eluted with a gradient from 10-400 mM imidazole (over 16 column volumes), collecting 5-ml fractions. Fractions containing the GFP-HsFTVI were pooled and exchanged into a storage buffer (25 mM Tris pH 7.5, 150mM NaCl) using a desalting column (GE Healthcare). Protein was concentrated using a 30-KDa MW cutoff Amicon Ultra centrifugal filter unit (Millipore), frozen in liquid nitrogen and stored at -80°C. The final yield was 5.5 mg of GFP-HsFTVI per liter of cell culture supernatant. This protein was used for Saturation Transfer Difference (STD) NMR experiments.

Saturation Transfer Difference (STD) NMR experiments

All experiments were performed using a "Bruker Avance I" 500 MHz spectrometer with a 5 mm PATXI 1H/D-13C/15N Z-GRD probe at a temperature of 285 K. For assignment, mimetic **1** was prepared at 1 mM concentrations in 25 mM Tris-d11, 150 mM NaCl buffer in D₂O at pH 7.5. Assignments were completed using standard 1H-13C HSQC (*hsqcetgpsi*) and COSY (*cosygpmfph*) experiments. STD NMR samples were prepared with 1.0 mM concentration of **1** and 25 μ M of FTVI in 25 mM Tris-d11, 150 mM NaCl buffer in D₂O at pH 7.5. STD NMR experiments were performed using the residual water peak as a reference for chemical shifts and at saturation times (d20) of 0.5 s, 1 s, 2 s, 3 s, 4 s and 5 s with a recycle delay (d1) of 5 s. A train of 50 ms, 1.1 mW Gaussian pulses applied at -1 ppm (on-resonance) or 40 ppm (off-resonance) on the f2 channel were used. To remove unwanted x,z signals a spoil sequence was used composing of 2 trim pulses of 2.5 ms and 5 ms, followed by a 40% z-gradient for 3 ms. To supress protein signals a spin lock of 0.9 W for 40 ms was used. STD NMR competition experiments with GDP were run on the previously produced STD NMR sample containing FTVI and **1**, by addition of a concentrated GDP stock, to achieve a GDP concentration of first 1 mM, and then 10 mM. STD NMR competition experiments with GDP-fucose were run on a sample prepared in the exact same conditions as the previous, but with another batch of FTVI coming in 25 mM Tris-d11, 150 mM NaCl in D₂O at pH 7.5, which produced lower STD (%) (Fig. 2d). The *stddiffgp19.3* pulse sequence was used. All competition experiments were run at a saturation time (d20) of 2 s.

Saturation Transfer Difference (STD) NMR experiments. Binding Epitope Mapping from Initial Slopes (STD build-up curves)

STD build-up curves were constructed for each proton of **1** by measuring the STD intensity at a number of saturation times (0.5, 1, 2, 3, 4, 5 s). This allowed the initial rate of STD build-up (STD_0) to be calculated by performing a least-squares fitting of the following mono-exponential curve:

$$STD(t_{sat}) = STD_{max}(1 - \exp(-k_{sat}t_{sat}))$$

where $STD(t_{sat})$ is the STD intensity for a saturation time, t_{sat} , STD_{max} is the maximum STD intensity, and k_{sat} is the rate constant for saturation transfer. In the limit, $t_{sat} \rightarrow 0$:

$$STD_0 = STD_{max}k_{sat}$$

Importantly, STD_0 gives a value that is independent of any relaxation or rebinding effects, allowing for a more accurate binding epitope.⁷ The value of STD_0 was then normalised against

the proton with the largest intensity (Ha) to give values in the range of 0-100 %, which were then mapped on to a ligand structure to give the binding epitope (Figure 2b, main text).

Table S1. Normalised STD_0 values for 1. Table showing normalised values of STD_0 (column “Relative STD”) for each proton of the inhibitor 1. The values of STD_0 (column “Initial Slope”) were normalised against the largest value for each ligand. The second column shows the values of the parameters STD_{max} and k_{sat} obtained by fitting the experimental STD data to the monoexponential equation described above.

Proton		Initial Slope	Relative STD
H1	STD_{max}	27.37	31.78
	k_{sat}	1.16	
H2	STD_{max}	19.67	22.05
	k_{sat}	1.12	
H3	STD_{max}	16.29	22.97
	k_{sat}	1.41	
H4	STD_{max}	16.93	25.89
	k_{sat}	1.53	
H5	STD_{max}	17.55	27.76
	k_{sat}	1.58	
H6	STD_{max}	12.07	33.92
	k_{sat}	2.81	
Hb	STD_{max}	29.26	36.92
	k_{sat}	1.26	
Ha	STD_{max}	31.77	38.25
	k_{sat}	1.20	
Hc	STD_{max}	25.00	26.32
	k_{sat}	1.05	
CH2	STD_{max}	13.71	22.61
	k_{sat}	1.65	

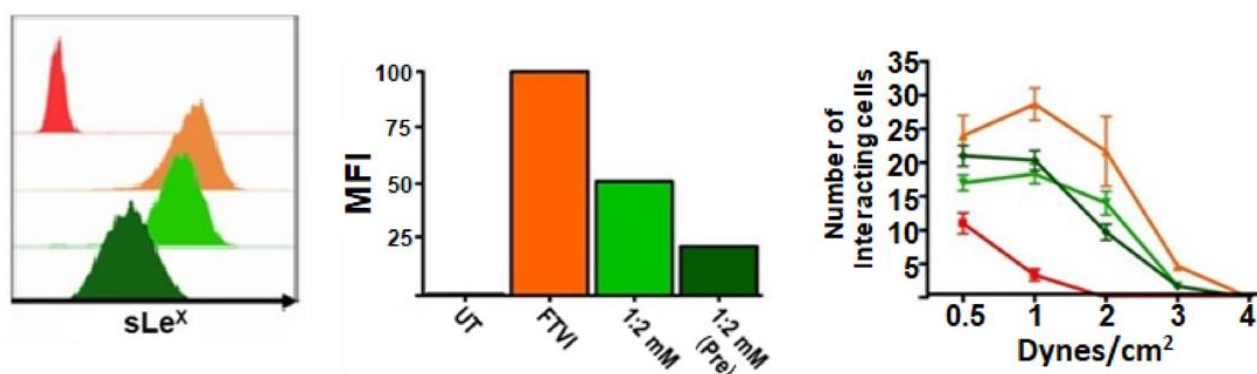


Figure S5. RPMI-8402 cell line was untreated (red), exofucosylated with 1.0 mM GDP-Fuc (orange), 1.0 mM GDP-Fuc to 2.0 mM 1 (light green), or preincubated with FTVI and 1 (2.0 mM) for 45 min followed by addition of GDP-Fuc (1.0 mM) for 1 h (dark green). RPMI-8402 subsets were then loaded into chambers containing monolayers of E-selectin bearing HUVECs with an initial shear rate of 0.5 dyne/cm², with shear incremented stepwise until 8 dynes/cm². The number of RPMI-8402 cell tethering/interactions were quantified at each shear rate and averaged across three different fields of view.

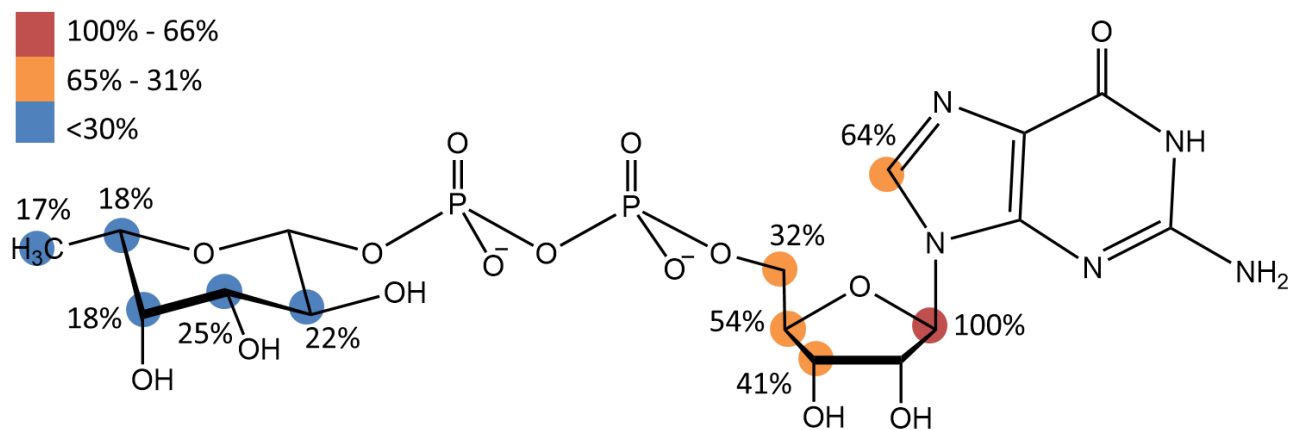


Figure S6. Binding epitope mapping for the interaction of the donor substrate GDP-fucose to FTVI as obtained by STD NMR build-up curves.

Dynamic light scattering (DLS)

DLS measurements were carried out on a Brookhaven instrument (a BI 9000AT correlator and a BI200 SM goniometer), equipped with a Peltier temperature control system. The light source was a Torus laser, mpc3000, Laser Quantum, UK ($\lambda = 532$ nm) and the scattered intensity was detected using a BI-APD detector. All DLS curves were acquired at 25°C. DLS measurements were performed on 1.0 mM solution of mimetic **1** (25 mM TRIS, 150 mM NaCl, pH 7.5).

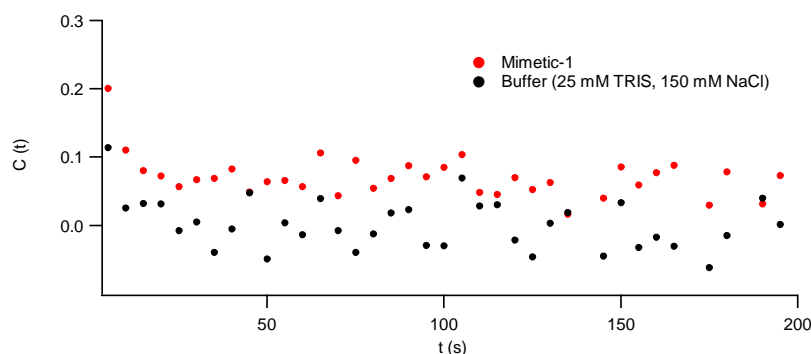


Figure S7. Representative correlograms of mimetic **1** solution and buffer, showing no signal correlation within 2 minutes of measurement. No significant difference was observed between the recorded scattering intensity of the sample and the buffer (*i.e.* 1.7 kcps and 2.5 kcps, respectively), indicating the absence of nano or micrometric aggregates within the sample. As a further confirmation, the scattering signal of the 1.0 mM solution of mimetic **1** does not correlate with itself in the time scale of the experiment (2 minutes of recorded scattering intensity), as in the case of buffer.

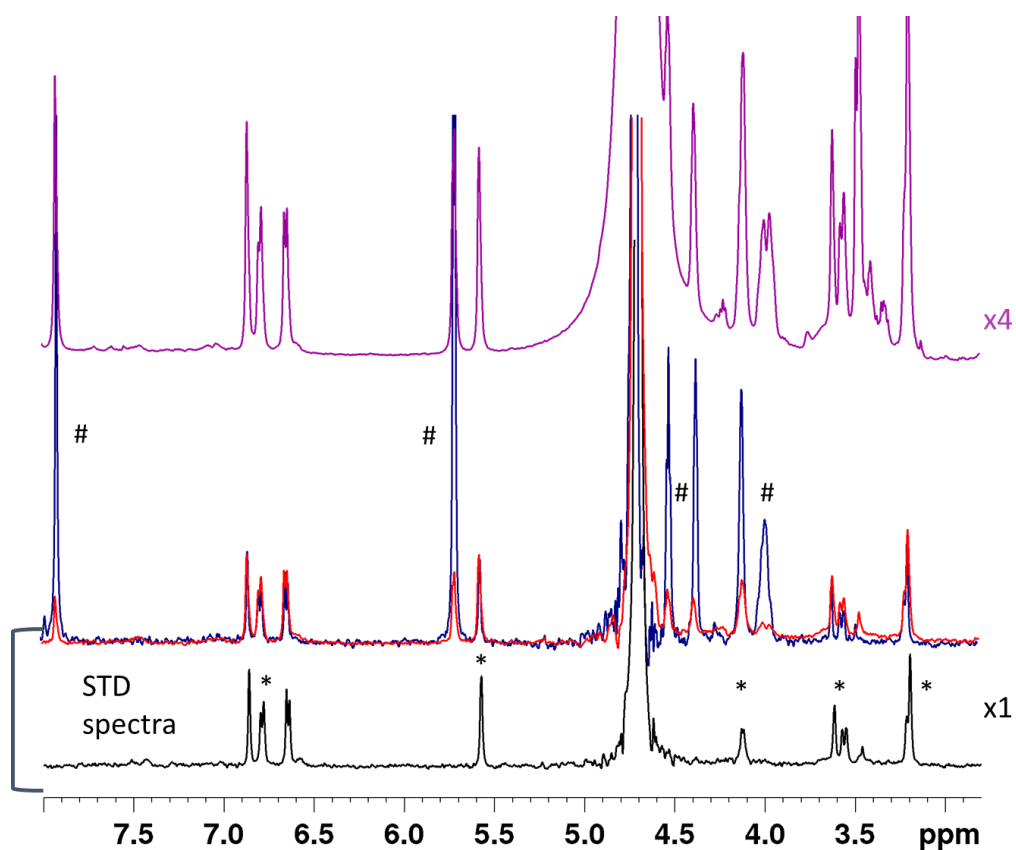


Figure S8. STD NMR competition experiments of mimetic **1** with GDP for binding to FTVI. The reference spectra of the sample containing 1.0 mM of mimetic **1** and 1.0 mM GDP is shown on top, in purple at 4x magnification (reference spectra of the sample containing 1.0 mM mimetic **1**, and 1.0 mM mimetic **1** + 10 mM GDP are not shown, to avoid figure over-crowding). The STD spectra of the sample containing 1 mM mimetic **1** (black), 1.0 mM mimetic **1** + 1.0 mM GDP (red) and 1 mM mimetic **1** + 10 mM GDP (blue) are shown on the bottom, all at 1x magnification. The mimetic **1** signals are labelled with a star (*), while the GDP signals are labelled with an hash (#).

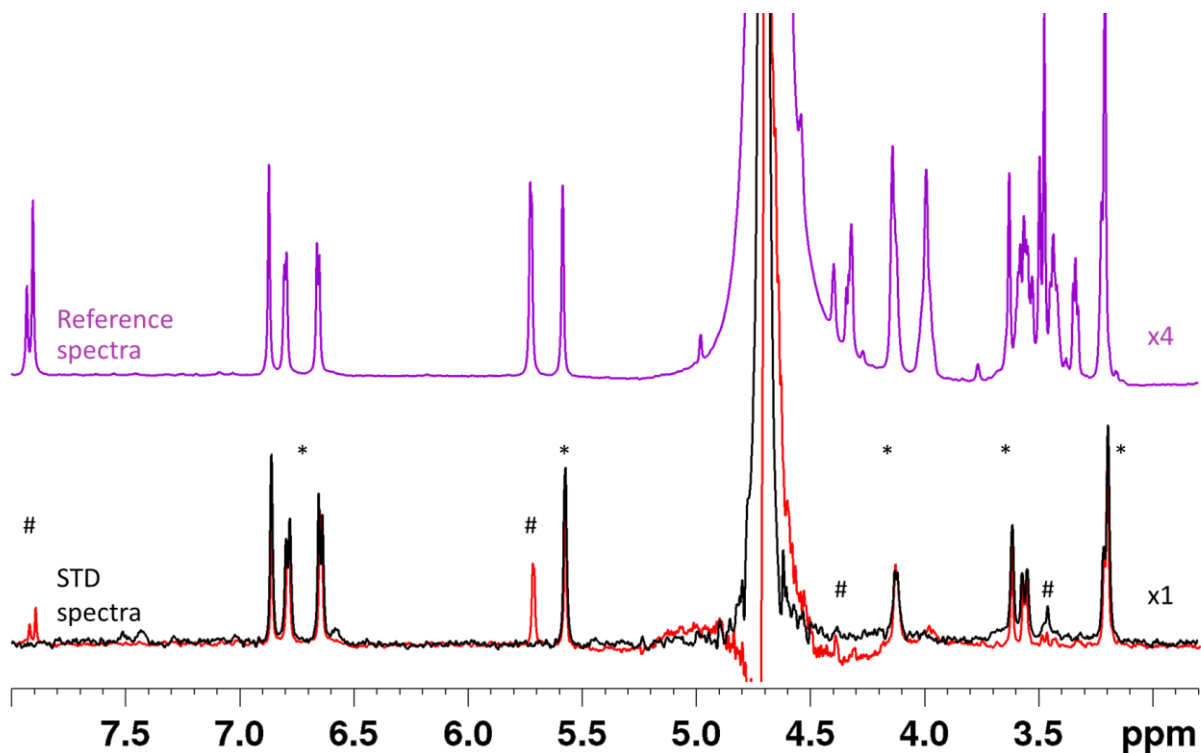


Figure S9. STD NMR competition experiments of mimetic **1** with GDP-fucose for binding to FTVI. The reference spectra of the sample containing 1 mM of mimetic **1** and 1.0 mM GDP-fucose is shown on top, in purple at 4x magnification (reference spectra of the sample containing 1.0 mM mimetic **1** is not shown, to avoid figure over-crowding). The STD spectra of the sample containing 1 mM mimetic **1** (black) and 1.0 mM mimetic **1** + 1.0 mM GDP-fucose (red) are shown on the bottom, at 1x magnification. The mimetic **1** signals are labelled with a star (*), while the GDP-fucose signals are labelled with an hash (#).

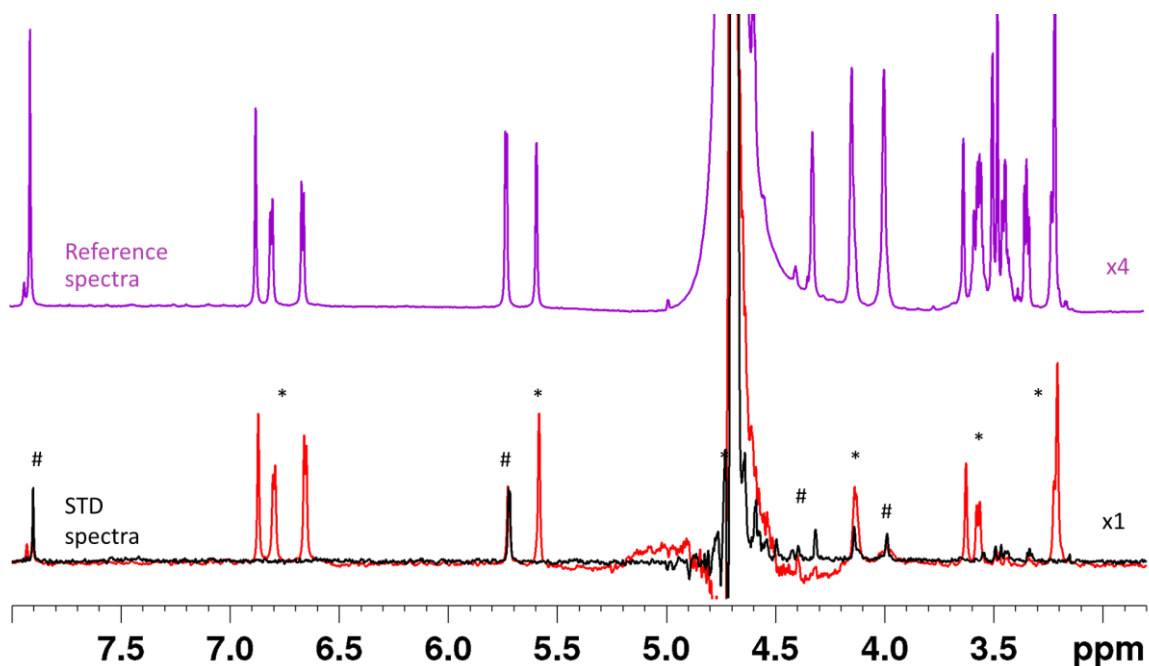


Figure S10. STD NMR competition experiments of GDP-fucose upon addition of mimetic **1** for binding to FTVI. The reference spectra of the sample containing 1.0 mM of mimetic **1** and 1.0 mM GDP-fucose is shown on top, in purple at 4x magnification (reference spectra of the sample containing 1 mM GDP-fucose is not shown, to avoid figure over-crowding). The STD spectra of the sample containing 1 mM GDP-fucose (black) and 1.0 mM GDP-fucose + 1.0 mM mimetic **1** (red) are shown on the bottom, at 1x magnification. The mimetic **1** signals are labelled with a star (*), while the GDP-fucose signals are labelled with an hash (#).

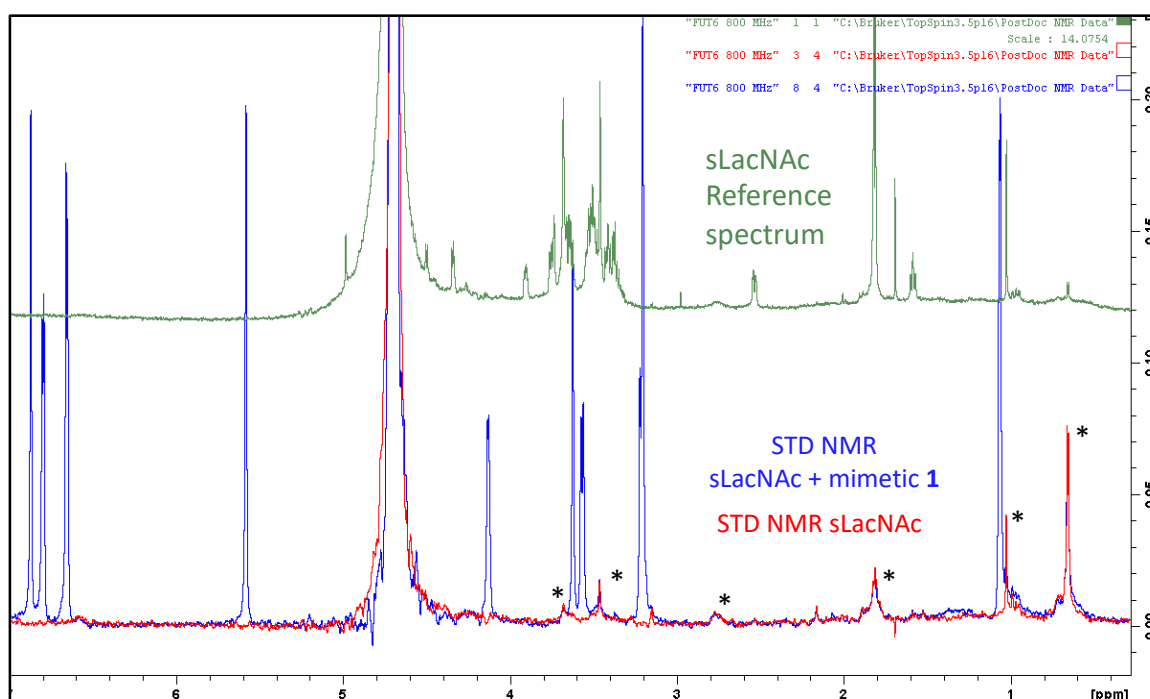


Figure S11. STD NMR competition experiments of sLacNAc upon addition of mimetic **1** for binding to FTVI. The reference spectra of the sample containing 1.0 mM of sLacNAc is shown on top (green). At the bottom, in red, the STD NMR spectrum of sLacNAc in the presence of FTVI showed no signals from the ligand (only residual baseline signals from the protein were observable, labelled with asterisks). Upon addition of 1.0 mM mimetic **1**, no change in the baseline residual signals was observed, and intense STD NMR signals from mimetic **1** were observable (blue), reporting binding of the latter. Unfortunately the absence of sLacNAc STD NMR signals precludes any interpretation regarding potential competition with mimetic **1**.

References

1. D.A. Case, S.R. Brozell, D.S. Cerutti, Cheatham, T.E. III, Cruzeiro, V.W.D.; Darden, T.A.; Duke, R.E.; Ghoreishi, D.; Gohlke, H.; Goetz, A.W.; Greene, D.; Harris, R.; Homeyer, N.; Izadi, S.; Kovalenko, A.; Lee, T.S.; LeGrand, S.; Li, P.; Lin, C.; Liu, J.; Luchko, T.; Luo, R.; Mermelstein, D.J.; Merz, K.M.; Miao, Y.; Monard, G.; Nguyen, H.; Omelyan, I.; Onufriev, A.; Pan, F.; Qi, R.; Roe, D.R.; Roitberg, A.; Sagui, C.; Schott-Verdugo, S.; Shen, J.; Simmerling, C.L.; Smith, J.; Swails, J.; Walker, R.C.; Wang, J.; Wei, H.; Wolf, R.M.; Wu, X.; Xiao, L.; York D.M.; Kollman P.A. (2018), AMBER 2018, University of California, San Francisco.
2. J. Wang, R. M. Wolf, J. W. Caldwell, P. A. Kollman and D. A. Case, *J. Comput. Chem.*, **2004**, *25*, 1157–1174.
3. C. I. Bayly, P. Cieplak, W. Cornell and P. A. Kollman, *J. Phys. Chem.*, **1993**, *97*, 10269–10280.
4. Gaussian 09, Revision A.02, M. J. Frisch, G. W. Trucks, H. B. Schlegel, G. E. Scuseria, M. A. Robb, J. R. Cheeseman, G. Scalmani, V. Barone, G. A. Petersson, H. Nakatsuji, X. Li, M. Caricato, A. Marenich, J. Bloino, B. G. Janesko, R. Gomperts, B. Mennucci, H. P. Hratchian, J. V. Ortiz, A. F. Izmaylov, J. L. Sonnenberg, D. Williams-Young, F. Ding, F. Lipparini, F. Egidi, J. Goings, B. Peng, A. Petrone, T. Henderson, D. Ranasinghe, V. G. Zakrzewski, J. Gao, N. Rega, G. Zheng, W. Liang, M. Hada, M. Ehara, K. Toyota, R. Fukuda, J. Hasegawa, M. Ishida, T. Nakajima, Y. Honda, O. Kitao, H. Nakai, T. Vreven, K. Throssell, J. A. Montgomery, Jr., J. E. Peralta, F. Ogliaro, M. Bearpark, J. J. Heyd, E. Brothers, K. N. Kudin, V. N. Staroverov, T. Keith, R. Kobayashi, J. Normand, K. Raghavachari, A. Rendell, J. C. Burant, S. S. Iyengar, J. Tomasi, M. Cossi, J. M. Millam, M. Klene, C. Adamo, R. Cammi, J. W. Ochterski, R. L. Martin, K. Morokuma, O. Farkas, J. B. Foresman, and D. J. Fox, Gaussian, Inc., Wallingford CT, 2016.
5. T. A. Andrea, W. C. Swope and H. C. Andersen, *J. Chem. Phys.*, **1983**, *79*, 4576–4584.
6. T. Darden, D. York and L. Pedersen, *J. Chem. Phys.*, **1993**, *98*, 10089–10092.
7. J. Angulo, P.M. Enriquez-Navas and P.M. Nieto, *Chem. Eur. J.*, **2010**, *16*, 7803-7812.

Author Contributions

BR and RS designed the research in collaboration with: RHG in charge of biophysical data (data not shown) and FTVI expression, FC in charge of docking calculations and MD simulations, JA in charge of STD-NMR experiments. KCM, JT, AGG, LCL, TH, and SM performed the research. BR, RS, KCM, RHG, FC, and JA analyzed data. BR and RS wrote the paper.

BR and RS are co-last and co-corresponding authors.

Acknowledgements

We thank COST action CA18103 INNOGLY: INNOVation with GLYcans: new frontiers from synthesis to new biological targets. We thank Professor Kelly Moremen (University of Georgia) for supplying the pGEn2-HsFUT6 plasmid. We thank Dr. Lucrezia Caselli (Department of Chemistry, University of Florence) for DLS measurements. B.R. and J.T. thank MIUR-Italy ("Progetto Dipartimenti di Eccellenza 2018-2022" allocated to Department of Chemistry "Ugo Schiff"). F.C. Ministerio de Ciencia, Innovación y Universidades (RTI2018-099592-B-C21). S.M. was supported by the Biotechnology and biological Sciences Research Council (BBSRC)

through a New Investigator grant awarded to J.A. (BB/P010660/1). J.A. also acknowledges financial support from the Universidad de Sevilla (Acciones Especiales del VI Plan Propio de Investigación y Transferencia). T.H. thanks the BBSRC for a studentship as part of the Norwich Research Park Doctoral Training Partnership. We acknowledge access to UEA Faculty of Science Research Facilities. We thank Warrior Therapeutics LLC for gift of enzymes, and ARAID, MEC (CTQ2013-44367-C2-2-P, BFU2016-75633-P and PID2019-105451GB-10) and Gobierno de Aragón (E34_R17 and LMP58_18) with FEDER (2014-2020) funds for "Building Europe from Aragón" for financial support. This study was also funded by the US National Institutes of Health/National Cancer Institute (NCI) grant U01 CA225730-01 (to RS).

Abbreviations List

FTs: Fucosyltransferases; GDP-Fuc: Guanosine diphosphate fucose; Le^x: Lewis X; sLe^x: Sialyl Lewis X; LacNAc: Gal-β(1,4)-GlcNAc-α-1-R; sLacNAc: NeuAc-α(2,3)-Gal-β(1,4)-GlcNAc-α-1-R; RPMI-8402: Human lymphoblastic leukemia cells; MSCs: Human mesenchymal stem cells; UT: Untreated; Pre: Preincubation; HUVEC: Human umbilical vein endothelial cells; TNF: Tumor necrosis factor; STD: Saturation transfer difference; GFP: Green fluorescent protein; DLS: Dynamic Light Scattering